

The Fermi surface of underdoped high- T_c superconducting cuprates

Xi Dai,^a Zhao-bin Su,^a and Lu Yu^{b,a}

^a *Institute of Theoretical Physics, Academia Sinica, P.O. Box 2735, Beijing 100080, China*

^b *International Center for Theoretical Physics, P.O. Box 586, Trieste 34100, Italy*

Abstract

The coexistence of π -flux state and d-wave RVB state is considered in this paper within the slave boson approach. A critical value of doping concentration δ_c is found, below which the coexisting π -flux and d-wave RVB state is favored in energy. The pseudo Fermi surface of spinons and the physical electron spectral function are calculated. A clear Fermi-level crossing is found along the (0,0) to (π, π) direction, but no such crossing is detected along the $(\pi, 0)$ to (π, π) direction. Also, an energy gap of d-wave symmetry appears at the Fermi level in our calculation. The above results are in agreement with the angle-resolved photoemission experiments which indicate at a d-wave pseudo-gap and a half-pocket-like Fermi surface in underdoped cuprates.

PACS Numbers: 71.27.+a, 71.10.Pm, 71.10.Hf

Key words: pseudo-gap, Fermi surface, d-wave RVB state, flux phase

Category: Ca2

Contact Author: Xi Dai

Mailing Address: Institute of Theoretical Physics, P.O. Box 2735, Beijing 100080,
P. R. of China

E-mail: daix@sun.itp.ac.cn

I. INTRODUCTION

A great deal of attention has been focused on the studies of the electronic structure of the high T_c superconducting cuprates (HTSC) in the past decade [1–3]. In the undoped case, the charge mobility is suppressed by the strong on-site Coulomb repulsion and the spin- $\frac{1}{2}$ antiferromagnetic Heisenberg model is believed appropriate to describe the electronic properties of these materials [2]. In the opposite limit, when the cuprates are overdoped in the copper-oxide plane, the HTSC is metallic and the observed electronic structure is in good agreement with predictions of the local density approximation (LDA) calculations [4]. In-between these two limits, many interesting phenomena appear including superconductivity. The evolution of the electronic structure from one limit to another should play a key role for the understanding of numerous anomalous properties of HTSC discovered in this doping range.

When slightly doped with holes in the antiferromagnetic Cu-O plane, the Fermi surface of the mobile holes is expected to be small pockets centered at $(\pm\pi/2, \pm\pi/2)$. On the contrary, in the overdoped case the Fermi surface should be a large one centered at (π, π) as reported by both angle-resolved photo-emission spectroscopy (ARPES) experiments [5] and the LDA calculations [4]. However, the crossover from one limit to another is not well understood yet.

The recent ARPES experiments [6–8] on underdoped samples seem to indicate that the Fermi surface of these compounds is probably half-pocket-like, *i.e.* a small pocket near $\Sigma(\pi/2, \pi/2)$, but lacking its outer part in the reduced Brillouin zone scheme (see the dashed line in Fig. 3). The data of Marshall *et al.* [6,7] show a well defined Fermi-level crossing along the $(0, 0)$ to (π, π) direction, but no such crossing has been detected along the $(\pi, 0)$ to (π, π) direction. This result differs substantially from that of the optimally doped samples which exhibit a large Fermi surface with well defined Fermi-level crossing in both $(0, 0)$ to (π, π) and $(\pi, 0)$ to (π, π) directions.

Another puzzling phenomenon in underdoped cuprates is the presence of a pseudo-gap

in the normal state. Both Stanford [7] and Argonne [8] groups have shown strong evidence for the suppression of the density of states near the Fermi level indicating at the formation of the pseudo-gap. Several different measurements, including specific heat and thermal power [9,10], Hall coefficient [11], and transport [12], as well as nuclear magnetic resonance (NMR) [13] and neutron scattering experiment [14], have also shown the presence of the pseudo-gap in underdoped cuprates. The symmetry of the pseudo-gap has been found d-wave like [7,8] with a maximum value in the $(\pi, 0)$ to (π, π) direction, and it is very much reduced in the $(0, 0)$ to (π, π) direction. This result is also consistent with earlier data of Marshall *et al.* [6], where dramatical changes have been observed for the spectral density near $(0, \pi)$.

Theoretically, the origin of the pseudo-gap can be ascribed either to short range AF fluctuations in the weak coupling approach [15] or to d-wave pairing of spinons [16,17] in the resonant valence bond (RVB) state [18]. Due to the SU(2) symmetry at half filling, the d-wave and s+id wave [19] RVB states, as well as π flux state [20] are degenerate [21]. Away from half filling, the commensurate flux phase (CFP) [22], the staggered flux phase (SFP) [23] and the d-wave RVB state [24] are competing candidates for the ground state. Further study shows that the CFS is favoured only in the limit $t \ll J$ [22], which is not the actual case in cuprates. Zhang [24] has studied the competition and possible coexistence of the SFP and d-wave RVB state, and he concluded that SFP is unstable against d-wave RVB state and there is no coexistence of these two states at any non-half-fillings. However, Zhang's conclusion was based on the renormalized mean-field theory which satisfies the no-double occupancy constraint only on average. To improve the situation, in one of our earlier papers [25], D.N. Sheng and two of us (Z.B. Su and L. Yu) have reconsidered this issue using a better treatment of the slave-boson mean field theory, proposed by Nori, Abrahams and Zimanyi (NAZ) [26], transmuting the holons into spinless Fermions via a 2D Jordan-Wigner transformation. Using NAZ statistics transmutation trick it was found that the π -flux state can coexist with the s+id-wave RVB state below a critical doping δ_c , while the d-wave state takes over beyond that critical concentration.

Recently, a SU(2) slave boson theory was proposed by Wen and Lee [17], significantly

improving the earlier $U(1)$ version, especially for the underdoped systems. In their approach the $SU(2)$ symmetry is preserved away from half-filling by introducing two kinds of slave bosons. Considering the effective interaction between holons and spinons they obtain a small Fermi Surface in underdoped regime. We will elaborate further on their results later, comparing them with ours.

In the present paper we develop a slave boson approach for the $t - J$ model, with a more careful treatment of the hard-core constraint for the holons by transforming them into fermions. Following NAZ [26], a statistical gauge field A_{ij} is introduced to implement this transmutation. The effective gauge field seen by the holons will be a superposition of the π -flux contributed by the spinons and the statistical gauge field reflecting the hard-core nature of the holons. Using the equivalence of the π -staggered and π -uniform flux, we find that the statistical gauge field can substantially compensate the π -flux. Then the effective flux acting on holons satisfies the commensurability condition which minimizes the holon free energy. The mean field phase diagram is obtained and the coexisting d-wave RVB and π -flux state is found energetically more favourable with respect to the pure d-wave state in the underdoped region. This confirms the earlier result [25], and disagrees with Zhang's conclusion [24], excluding the coexistence of these two states. It appears to us that the main reason of this discrepancy is due to the fact that in Zhang's approach the holons and spinons are not treated on an equal footing. The dynamics of holons is basically ignored in his approach, leading only to the renormalization of the hopping integral. On the contrary, in our approach, the full dynamics of holons is considered and the holons and spinons are treated equally. (We will elaborate more on the differences of these two approaches in the concluding remarks.) Furthermore, we have calculated the physical electron spectral function in the low doping range and have found the half-pocket-like Fermi surface as well as the pseudo-gap in the same doping range. We emphasize that the pseudo-gap obtained in our approach opens right at the Fermi surface and therefore it is consistent with the ARPES experiments. Thus our calculation can very well explain the APRES results without invoking the additional (not physical) $SU(2)$ symmetry away from half-filling.

The rest of the paper is organized as follows: The mean field theory is given in Sec. II, whereas the spectral function for the physical electron is presented in Sec. III. Finally, we make a few concluding remarks in Sec. IV.

II. MEAN FIELD THEORY OF THE $t - J$ MODEL

We begin with the slave boson representation of the $t - J$ model in which the physical electron destruction operator $c_{i\sigma}$ is represented in terms of the pseudo-fermion operator $f_{i\sigma}$ and the slave boson operator b_i^+ as $c_{i\sigma} = f_{i\sigma}b_i^+$. The partition function reads as :

$$Z = \int \prod_{i\sigma} D[f_{i\sigma}^+(\tau)] D[f_{i\sigma}(\tau)] D[b_i^+(\tau)] D[b_i(\tau)] \exp[-\int_0^\beta L d\tau] \quad (1)$$

with

$$\begin{aligned} L = & \sum_{i\sigma} f_{i\sigma}^+(\tau) \left(\frac{\partial}{\partial \tau} - \mu_2 \right) f_{i\sigma}(\tau) + \sum_i b_i^+(\tau) \left(\frac{\partial}{\partial \tau} - \mu_1 \right) b_i(\tau) + N\mu_1\delta + N\mu_2(1-\delta) \\ & - \frac{1}{2} \sum_{\langle ij \rangle} (\tau_{ij} + t b_i^+ b_j) (\tau_{ji} + t b_j^+ b_i) - \frac{t^2}{2} \sum_{\langle ij \rangle} b_i^+ b_i b_j^+ b_j + \frac{t^2}{2} \sum_i b_i^+ b_i \\ & - \frac{1}{2} \sum_{\langle ij \rangle} \Delta_{ij}^+ \Delta_{ij} + t' \sum_{(ii')} f_{i\sigma}^+ f_{i'\sigma} b_i b_{i'}^+, \end{aligned} \quad (2)$$

where we define

$$\tau_{ij} = \sum_{\sigma} f_{i\sigma}^+ f_{j\sigma}, \quad \Delta_{ij} = \sum_{\sigma} \sigma f_{i\sigma} f_{j\bar{\sigma}}.$$

The chemical potentials for the boson μ_1 and the fermion μ_2 are chosen to satisfy the global constraints $n_f + n_b = 1$ and $n_b = \delta$, with δ as the doping concentration. We take the exchange integral $J = 1$, while t , t' are the nearest neighbor, and next nearest hopping terms, respectively. Hereafter $\langle ij \rangle$ means nearest neighbor, while (ii') means next nearest summation. N is the total number of sites, and β is the inverse temperature.

We introduce the Hubbard-Stratonovich (HS) transformation:

$$\begin{aligned}
Z = & \int \prod_{i\sigma} D[f_{i\sigma}^+] D[f_{i\sigma}] D[b_i^+] D[b_i] \prod_{\langle ij \rangle} D[\chi_{ij}^*] D[\chi_{ij}] D[D_{ij}^*] D[D_{ij}] \\
& \cdot \prod_{\langle ii' \rangle} D[\rho_{ii'}^*] D[\rho_{ii'}] \exp[-\int_0^\beta L'(\tau) d\tau]
\end{aligned} \tag{3}$$

with

$$\begin{aligned}
L'(\tau) = & \sum_{i\sigma} f_{i\sigma}^+(\tau) \left(\frac{\partial}{\partial \tau} - \mu_1 \right) f_{i\sigma}(\tau) + \sum_i b_i^+(\tau) \left(\frac{\partial}{\partial \tau} - \mu_2 \right) b_i(\tau) + \frac{1}{2} \sum_{\langle ij \rangle} \chi_{ij}^*(\tau) \chi_{ij}(\tau) \\
& + \frac{1}{2} \sum_{\langle ij \rangle} D_{ij}^*(\tau) D_{ij}(\tau) - t' \sum_{\langle ii' \rangle} \rho_{ii'}^*(\tau) \rho_{ii'}(\tau) - \frac{1}{2} \sum_{\langle ij \rangle \sigma} \left[\chi_{ij}^*(\tau) f_{i\sigma}^+(\tau) f_{j\sigma}(\tau) + h.c. \right] \\
& - \frac{1}{2} \sum_{\langle ij \rangle \sigma} \left[D_{ij}^*(\tau) \Delta_{ij} + h.c. \right] - \frac{t}{2} \sum_{\langle ij \rangle} (\chi_{ij}^* b_i^+ b_j + h.c.) + t' \sum_{\langle ii' \rangle \sigma} \left[\rho_{ii'}^* f_{i\sigma}^+ f_{i'\sigma} + h.c. \right] \\
& + t' \sum_{\langle ii' \rangle} \left[\rho_{ii'} b_i^+ b_{i'} + h.c. \right] - \frac{t^2}{2} \sum_{\langle ij \rangle} b_i^+ b_i b_j^+ b_j + \frac{t^2}{2} \sum_i b_i^+ b_i + \mu_1 \sum_i \delta + \mu_2 \sum_i (1 - \delta).
\end{aligned} \tag{4}$$

In the saddle point approximation of the above action, we treat the amplitudes of the HS fields D_{ij} , χ_{ij} and $\rho_{ii'}$ as site- and time-independent with some phase factors, namely,

$$D_{ij}(\tau) = \Delta \eta_{ij}, \quad \chi_{ij}(\tau) = p \exp(i\phi_{ij}), \quad \rho_{ii'}(\tau) = \rho$$

with

$$\eta_{ij} = \begin{cases} 1 & (\hat{j} = \hat{i} \pm \hat{x}), \\ -1 & (\hat{j} = \hat{i} \pm \hat{y}), \end{cases}$$

while ϕ_{ij} is the phase factor in the Affleck-Marston flux phase [20] to be described in detail later.

We then obtain the mean-field Hamiltonian per site as:

$$\begin{aligned}
H_{MF} = & H_c + H_s + H_h, \\
H_c = & \frac{1}{2} \Delta^2 + \frac{1}{2} p^2 + \mu_2 (1 - \delta) + \mu_1 \delta - \frac{t^2}{2} \delta (\delta - 1) + t' |\rho|^2, \\
H_s = & -\frac{p}{2N} \sum_{\langle ij \rangle \sigma} (e^{i\phi_{ij}} f_{i\sigma}^+ f_{j\sigma} + h.c.) - \frac{\Delta}{2N} \sum_{\langle ij \rangle \sigma} \left[\eta_{ij\sigma} f_{i\sigma}^+ f_{j\bar{\sigma}}^+ + h.c. \right]
\end{aligned}$$

$$\begin{aligned}
& + \frac{t'\rho}{N} \sum_{(ii')\sigma} (f_{i\sigma}^+ f_{i'\sigma} + h.c.) - \frac{\mu_2}{N} \sum_{i\sigma} f_{i\sigma}^+ f_{i\sigma} \\
H_h = & - \frac{tp}{2N} \sum_{\langle ij \rangle} (e^{i\phi_{ij}} b_i^+ b_j + h.c.) + \frac{t'\rho}{N} \sum_{(ii')} (b_i^+ b_{i'} + h.c.) - \frac{\mu_1}{N} \sum_i b_i^+ b_i. \quad (5)
\end{aligned}$$

We introduce a statistical gauge field operator A_{ij} to account for the hard-core nature of the holons, namely, $b_i^+ b_j = \exp(iA_{ij}) h_i^+ h_j$, with h_i^+ , h_j as fermion operators. In the mean field approximation, the statistical field A_{ij} is considered as a c-number, but it must obey the constraint:

$$\sum_{\text{plaquette}} A_{ij} = 2\pi(2q+1)\delta$$

with q as an integer., This constraint can be satisfied by introducing an additional uniform flux attached to the holons. Then the effective mean field Hamiltonian for holons reads as :

$$H_h = -\frac{tp}{2N} \sum_{\langle ij \rangle} [e^{i(\phi_{ij}+A_{ij})} h_i^+ h_j + h.c.] - \frac{t'\rho}{2N} \sum_{(ii')} [e^{i(\phi_{ii'}+A_{ii'})} h_i^+ h_{i'} + h.c.] - \frac{\mu_1}{N} \sum_i h_i^+ h_i. \quad (6)$$

The effective flux that acts on the holons is then :

$$\Phi_h = \sum_{\text{plaquette}} (A_{ij} + \phi_{ij}) + 2\pi k = 2\pi\delta + 4\pi q\delta + 2\pi k + \pi,$$

where k is an integer. If $\delta = (2p_1 - 1)/4k_1$, we can choose proper q_1 and k_1 to satisfy the commensurability condition $\Phi_h = 2\pi\delta$ which minimizes the total free energy of holons . In the present calculation we choose $k_1 = 25$ and $p_1 = 1, 2, \dots, 25$, so the above commensurability condition is always satisfied. Thus we transform the holon Hamiltonian into a simple form equivalent to the problem of noninteracting lattice fermions moving in a uniform magnetic field. We then diagonalize this mean field Hamiltonian of holons by solving the well-known Harper's equation.

For the spinon Hamiltonian we choose a proper gauge shown in Fig. 1, where $\phi_{ij} = \frac{\pi}{4}$ if R_{ij} is along the arrow shown in the figure and $\phi_{ij} = -\frac{\pi}{4}$ in the opposite case. Then we divide the original lattice into two sublattices, labeled by 1 and 2. The spinon Hamiltonian written in the k -space is found to be:

$$H_s = -\frac{1}{N} \sum'_{k\sigma} (e(k) + \mu_2) f_{1k\sigma}^+ f_{1k\sigma} - \frac{1}{N} \sum'_{k\sigma} (e(k) + \mu_2) f_{2k\sigma}^+ f_{2k\sigma}$$

$$-\frac{1}{N} \sum'_k \frac{p}{\sqrt{2}} [(\gamma_+ + i\gamma_-) f_{1k\sigma}^+ f_{2k\sigma} + h.c.] + \sum'_k \Delta \gamma_- [f_{1k\uparrow}^+ f_{2-k\downarrow}^+ + h.c.], \quad (7)$$

where \sum' means summation over the reduced Brillouin zone with reciprocal vector $Q = (\pi, \pi)$,

$$\gamma_{\pm} = (\cos k_x \pm \cos k_y), \quad e(k) = 2t'\rho [\cos(k_x - k_y) + \cos(k_x + k_y)].$$

The above Hamiltonian can be diagonalised by the Bogoliubov transformation, and we obtain the quasi-particle energy as $\pm E_{ks}$, and with $s = \pm 1$:

$$E_{ks} = \left\{ \left[sp \sqrt{\frac{\cos^2(k_x) + \cos^2(k_y)}{2}} - \mu_2 - e(k) \right]^2 + \Delta^2 \gamma_-^2 \right\}^{1/2}. \quad (8)$$

Now we calculate the spinon and holon free energy for given values of p , δ , ρ , μ_1 and μ_2 . The parameters are chosen as $t = 2$, $t' = 0.2$, and the free energy is calculated at temperature $T = 0.05$. We minimize the total free energy by varying the order parameters p , Δ , ρ and μ to obtain the mean field phase diagram as a function of doping concentration. The spinon dispersion obtained by our approach shows that the pseudo-gap opens up right at the Fermi level which vanishes along the line $k_x = \pm k_y$ reflecting the d-wave symmetry.

As shown in Fig. 2, the coexistence of π -flux and d-wave RVB state is favored in energy in the low doping range, while in the high doping range the pure d-wave RVB state takes over. The critical value of the doping concentration is found to be near 0.3. We believe this phase diagram is correct only qualitatively, since the fluctuations around the saddle point have been ignored in our present study. This calculation has confirmed the earlier result [25]. The new ingredient here is to introduce the next nearest neighbor hopping t' which turns out to be essential for obtaining the correct shape of the spectral function. Like in the CFP [22], the mean field treatment of the commensurability condition $\Phi_h = 2\pi\delta$ for holons breaks the parity and time-reversal symmetry at arbitrary filling. However, this is an artifact due to the mean field treatment.

III. ELECTRON SPECTRAL FUNCTION

Now we calculate the spectral function for physical electrons. It is more convenient to use the boson representation for holons instead of the fermion representation because we can not fully restore the Bose statistical property of the holon operator in the mean field approximation when the operator A_{ij} is treated as a c-number. The boson representation for holons is a further approximation compared with the mean field treatment in the preceding Section. However, we do use the coexisting π -flux and d-wave RVB order parameters obtained there to calculate the electron spectral function. Presumably, the main physical consequences of the coexisting phase are still kept.

First diagonalize the holon Hamiltonian in this boson representation. After Fourier transformation Eq.(5) reads as :

$$H_h = -\frac{1}{N} \sum'_k (e(k) + \mu_1) b_{1k}^+ b_{1k} - \frac{1}{N} \sum'_k (e(k) + \mu_1) b_{2k}^+ b_{2k} - \frac{1}{N} \sum'_k \frac{tp}{\sqrt{2}} [(\gamma_+ + i\gamma_-) b_{1k}^+ b_{2k} + h.c.], \quad (9)$$

where the indices 1,2 represent the two sublattices defined above.

This Hamiltonian can be diagonalised as:

$$H_h = \frac{1}{N} \sum'_q E_b(q) (\beta_q^+ \beta_q - \alpha_q^+ \alpha_q) - \frac{\mu_1 + e(q)}{N} \sum'_q (\beta_q^+ \beta_q + \alpha_q^+ \alpha_q) \quad (10)$$

with

$$E_b(q) = \frac{pt}{\sqrt{2}} \sqrt{\cos^2(q_x) + \cos^2(q_y)},$$

which describes two kinds of free bosons labeled by α and β . At low temperatures, bosons occupy the low energy states. So we need to consider only the bottom of the lower band (the α band) near Γ point (0, 0). Expanding $E_b(q)$ near (0,0), we obtain the effective holon Hamiltonian as:

$$H_h = \sum_q \left(\frac{q^2}{2m_B} - \mu_B \right) \alpha_q^+ \alpha_q, \quad (11)$$

where μ_B is the renormalized boson chemical potential, and

$$\frac{1}{2m_B} = \frac{tp}{8} + 2t'\rho$$

The physical electron Green's function is:

$$G(k, \tau) = -\langle T_\tau (c_{k\sigma}(\tau) c_{k\sigma}^+(0)) \rangle, \quad (12)$$

where

$$c_{k\sigma} = \frac{1}{N} \sum_i c_{i\sigma} \exp(-ik \cdot R_i) = \frac{\sqrt{2}}{2} (c_{1k\sigma} + c_{2k\sigma}).$$

Hence

$$\begin{aligned} G(k, \tau) &= -\frac{1}{2} \sum_{\alpha, \beta} \langle T_\tau (c_{\alpha k\sigma}(\tau) c_{\beta k\sigma}^+(0)) \rangle \\ &= -\frac{1}{2} \sum_{\alpha, \beta, q} \langle T_\tau (f_{\alpha k+q\sigma}(\tau) f_{\beta k+q\sigma}^+(0)) \rangle \langle T_\tau (b_{\alpha q}^+(\tau) b_{\beta q}(0)) \rangle. \end{aligned} \quad (13)$$

We see that the physical electron Green's function in the slave-boson approximation is nothing but the fermion-boson polarization function. The spectral weight is thus:

$$\text{Im } G(k, \omega) = -\frac{1}{2N} \sum'_{\alpha\beta q\nu} S_{\alpha\nu}(k+q) S_{\beta\nu}^*(k+q) D_{\alpha 1}^*(q) D_{\beta 1}(q) \delta(\omega + \omega_q - \epsilon_{k+q}^\nu) [n_B(\omega_q) + n_f(\epsilon_{k+q}^\nu)], \quad (14)$$

where S and D are the transformation matrices used by us to diagonalize H_s and H_h , respectively. The first term of Eq. (14) contributes a quasiparticle like peak centered at $\epsilon_k^\nu - \mu_B$, being called the coherent part. The second term represents a featureless incoherent part extended over a wide range. The density of occupied states probed by ARPES is $\text{Im}G(k, \omega)n_f(\omega)$. If we consider only the holon states with low energies as discussed above, we find that the total spectral weight of the coherent part, detected by ARPES equals:

$$\begin{aligned} &\frac{1}{2N} \sum'_{\alpha\beta q\nu} \int d\omega S_{\alpha\nu}(k+q) S_{\beta\nu}^*(k+q) D_{\alpha 1}^*(q) D_{\beta 1}(q) \delta(\omega + \omega_q - \epsilon_{k+q}^\nu) n_B(\omega_q) n_f(\omega) \\ &\approx \frac{1}{2N} \sum'_{\alpha\beta q\nu} S_{\alpha\nu}(k) S_{\beta\nu}^*(k) D_{\alpha 1}^*(0) D_{\beta 1}(0) n_B(\omega_q) n_f(\epsilon_k) \\ &= \frac{1}{4N} \sum'_{\alpha\beta\nu} S_{\alpha\nu}(k) S_{\beta\nu}^*(k) \delta n_f(\epsilon_k) = \frac{1}{2} \langle f_{k\sigma}^+ f_{k\sigma} \rangle \delta = \frac{1}{2} n_s(k) \delta \end{aligned} \quad (15)$$

Since the spectral weight itself is proportional to $n_s(k)$, we conclude that the shape of the Fermi surface is approximatively determined by the spinon momentum distribution $n_s(k)$.

The width of the peak is roughly proportional to $T^{1/2}$, which is very similar to Lee and Nagaosa's [27] result for the uniform RVB phase.

Fig. 4 presents the momentum distribution of spinons in different directions (as defined in Fig. 3) within the slave boson approach. We see that the curve α which is along the direction (1,1), *i.e.* from (0, 0) to (π, π) , shows a clear step in the momentum distribution indicating at the Fermi-level crossing. However, away from the (1,1) direction, as shown by curves γ_1 and γ_2 , the step in the momentum distribution is smeared out by d-wave RVB order parameter, and the shadow band (the second peak beyond the Fermi surface) appears. Curve β shows the momentum distribution along the direction $(\pi, 0)$ to (π, π) , and there is no step detected, indicating the absence of Fermi-level crossing in that direction. The pseudo Fermi surface is plotted in Fig. 3 for $\delta=0.2$, appearing as an unclosed small pocket.

We then calculate the physical electron spectral function in the $\alpha, \beta, \gamma_1, \gamma_2$ four directions. The typical total spectral weight of α and γ_1 cuts, including both coherent and incoherent parts, is shown in Figs. 5-6. Fig. 5 shows the spectral weight along the α cut ((1,1) direction). We see the entire coherent part moving across the Fermi level in this direction, and no signature of an energy gap (depletion of spectral weight at the Fermi level) is noticed. In Fig. 6, the pseudo-gap is visible at the Fermi level, and the coherent part can still move entirely across the Fermi level. Along the γ_2 direction the pseudo-gap is bigger than what we find in Fig. 6., which reflects the d-wave symmetry. On the other hand, the spectral weight does not drop to zero abruptly, decreasing continuously as the k vector moves along the γ_2 direction. Finally, for the β cut we can hardly see any coherent part due to the small value of the spinon distribution $n_s(k)$, and the spectral weight is pushed down to the range much lower than the Fermi level, indicating at the formation of a maximal gap in this direction. Again, no abrupt Fermi-level crossing is detected along this direction. Our result is fully consistent with the ARPES data obtained by Loeser *et al.*, [7] which show a nearly perfect Fermi-level crossing along the α cut and no Fermi level crossing along the β cut. They could also find the pseudo-gap from their experimental data, with vanishing value along the α cut

and a maximum along the β cut. Similar results were also reported by H. Ding *et al.* [8].

In Wen and Lee's approach [17], the electron Fermi surface is determined by the pole of the renormalized electron Green's function due to interaction with the gauge field. An elliptical Fermi surface with strongly suppressed spectral weight on the outer edge is obtained in the low doping regime. This elliptic surface is not centered around Σ point, which is on the outer side and the wave function renormalization factor is exactly zero at that point. Hence there is no "shadow band" in their approach outside the boundary $(0, \pi) - (\pi, 0)$. A spin gap opens outside the small elliptical Fermi surface, but the gap is identically zero at the entire Fermi surface. Also, the quasiparticle peak crosses the Fermi level in all directions spanned by the Fermi surface. The main features of our results are similar to theirs, namely, small half-pocket-like Fermi surface near Σ , and d-wave like gap in the excitation spectrum. However, there are several important differences. In our approach the spinon Fermi surface is adjusted by the chemical potential, *i.e.* the doping concentration, so the d-wave like pseudo-gap is "locked" on the Fermi surface, and the pseudo-gap vanishes only at four points at which the Fermi surface intersects the line $k_x = \pm k_y$. As soon as the points of the Fermi surface slightly deviate from the $(1, \pm 1)$ direction, a finite energy gap appears. Also, the quasiparticle peak of the spectral function does not cross the Fermi level in any direction except for $(1, \pm 1)$. Another difference is we have small pockets centered around Σ and we do have shadow bands beyond the line $(0, \pi) - (\pi, 0)$. In principle, these different predictions can be checked by APRES experiments. It seems to us, however, that the presently available resolution is still not enough to resolve this issue.

IV. CONCLUDING REMARKS

Using the slave-boson approach, within the mean field approximation, we have shown in this paper that coexisting π -flux phase with d-wave RVB state is energetically more favorable in the low doping range (below δ_c), compared with the pure d-wave RVB state. We have also shown that this coexisting phase can provide a rather natural explanation for

the half-pocket-like small Fermi surface, a d-wave symmetry pseudo-gap, and very different behavior for the spectral function in the α and β directions, in underdoped HTSC. The main reason for this outcome is we have been able to better treat the single-occupancy constraint by introducing the additional statistical gauge field.

The advantage of a mean field approach compared with more sophisticated theories taking into account gauge field fluctuations is that it gives a more transparent understanding of the experimental results. When studying the problem of a single hole moving in the background of antiferromagnetic fluctuations, an effective hole band is obtained by both numerical and analytic methods. The hole band minimum is located at $(\pm\frac{\pi}{2}, \pm\frac{\pi}{2})$. Thus the Fermi surface of holes in the very low doping regime should be small pockets centered at $(\pm\frac{\pi}{2}, \pm\frac{\pi}{2})$ due to antiferromagnetic fluctuations. This conclusion is confirmed by the recent ARPES results. Hence the antiferromagnetic fluctuations leading to a bipartite lattice must be considered in the low doping regime. In our approach we introduce the π -flux phase which mimics the short range antiferromagnetic correlations which coexist with a weak d-wave RVB phase. Intuitively, the π -flux phase carries the physics of half-pocket-like Fermi surface while the coexisting d-wave phase is responsible for the pseudo-gap opened at the Fermi surface.

Zhang has concluded [24], however, that the π -flux state is unstable against the pure d-wave RVB state, excluding thus the possibility of their coexistence, using a renormalized mean field theory within the slave boson approach. What is the origin of the discrepancy between our result and his conclusion? We find that in the mean field theory of the $t-J$ model the total energy is divided into two parts. One is the kinetic energy which is characterized by the normal average terms $\langle f^+f \rangle$ (for spinon) and $\langle h^+h \rangle$ (for holons). The other is the exchange energy which is characterized by the anomalous average term $\langle f^+f^+ \rangle$. The π -flux state favors the kinetic energy, while the d-wave RVB state favors the exchange energy. In Zhang's approach the dynamical and statistical properties of holons which are shown to be nontrivial by our present study, are not considered, and the contribution of $\langle h^+h \rangle$ is ignored. This underestimates the kinetic energy gained by the delocalized mo-

tion of holons. Therefore the coexistence of π flux and the d-wave RVB state is excluded in Zhang's calculation. In our present study the dynamics of holons is fully considered, so we find that in the low doping regime the π -flux state coexisting with d-wave phase is more stable against both the pure π -flux state and the pure d-wave RVB state. The admixture of a small amount of the d-wave state will provide holons with more energy gain at the Fermi surface compared to the pure π -flux phase. Due to the smallness of the Fermi surface in the coexisting state the d-wave order parameter (of the order 0.1) is much smaller than the π -flux order parameter (of the order 1). The energy gap opens at the Fermi level due to the presence of the d-wave RVB order parameter. Since there is no Bose condensation in our calculation, this mixed state is responsible for the pseudo-gap in the normal state. With the increasing of the doping concentration, the area enclosed by the spinon Fermi surface is enlarged and the states near the Fermi surface take a higher percentage of the total occupied states and play a more important role compared with the low doping case. Therefore, in the high doping range, the d-wave RVB state gains free energy more effectively, and a crossover from the coexistence state to a pure d-wave state takes place. We believe our mean field treatment can serve as a good starting point for further improvement. It turns out that the mean field approximation of the $U(1) \times SU(2)$ Chern-Simons bosonization approach for the 2D $t - J$ model [30] leads to very similar results as the present study. The condensation of holons will lead to superconductivity which was not considered in this work. The fluctuations around the saddle point will create an effective attractive interaction between spinons and holons, as recently discussed by Wen and Lee [17]. The role of these fluctuations in our approach require further studies.

Very recently, Ding *et al.* [28] reported that there seems to be a large Fermi surface for HTSC over the entire range of doping, from underdoped to overdoped cases. However, their resolution is still not satisfactory for the substantially underdoped samples ($T_c = 15\text{K}$). It is yet to be seen how strong is their evidence. Also, the transport and optical data have shown rather strong evidence in favor of small hole pockets in the highly underdoped samples [29].

REFERENCES

- [1] E. Dagotto, *Revs. Mod. Phys.* **66**, 763 (1994).
- [2] A.P. Kampf, *Phys. Rep.* **249**, 219 (1994).
- [3] W. Brenig, *Phys. Rep.* **251**, 153 (1995).
- [4] W.E. Pickett, *Revs. Mod. Phys.* **61**, 433 (1989).
- [5] Z.X. Shen and D.S. Dessau, *Phys. Rep.* **253**, 1 (1995).
- [6] D.S. Marshall, D.S. Dessau, *et al.*, *Phys. Rev. Lett.* **76**, 4841 (1996).
- [7] A.G. Loeser, Z.X. Shen, *et al.*, *Science* **273**, 325 (1996).
- [8] H. Ding, T. Yokoya, *et al.*, *Nature (London)* **382**, 51 (1996).
- [9] J.W. Loram, K.A. Mirza, *et al.*, *Physic-a C* **235**, 134 (1994).
- [10] J.L. Tallon, J.R. Cooper, *et al.*, *Phys. Rev. Lett.* **75**, 4114 (1995).
- [11] H.Y. Hwang, *et al.*, *Phys. Rev. Lett.* **72**, 2636 (1994).
- [12] B. Batlogg, *et al.*, *Physica C* **235**, 130 (1994).
- [13] M. Takigawa, P.C. Hammel, *et al.*, *Phys. Rev. B* **43**, 247 (1991);
M. Takigawa, *ibid*, **49**, 4158 (1994); T. Imai, *et al.*, *Physica C* **162**, 169 (1989).
- [14] J. Rossat-Mignod, *et al.*, *Physica B* **169**, 58 (1991).
- [15] A.P. Kampf and J.R. Schrieffer, *Phys. Rev. B* **41**, 6399 (1990); A.V. Chubukov, D.K. Morr, and K.A. Shakhnovich, *Phil. Mag. B* **74**, 563 (1996).
- [16] H. Fukuyama, *Prog. Theor. Phys. Suppl.* **108**, 287 (1992)
- [17] X.G. Wen and P.A. Lee, *Phys. Rev. Lett.* **76**, 503 (1996)
see, also, P.A.Lee, N. Nagaosa, T.K. Ng, and X.G. Wen, Preprint cond-mat/9701168.

- [18] P.W. Anderson, Science **235**, 1196 (1987); G. Baskaran, Z. Zou, and P.W. Anderson, Solid State Commun. **63**, 973 (1987).
- [19] G. Kotliar, Phys. Rev. B **37**, 3664 (1988).
- [20] I. Affleck and J.B. Marston, Phys. Rev. B **37**, 3774 (1988).
- [21] I. Affleck, Z. Zhou, T. Hsu, and P.W. Anderson, Phys. Rev. B **38**, 745 (1988).
- [22] P. Lederer, D. Poilblanc, and T.M. Rice, Phys. Rev. Lett. **63**, 1519 (1989);
D. Poilblanc, Y. Hasegawa and T.M. Rice, Phys. Rev. B **41**, 1949 (1990);
S. Liang and N. Trivedi, Phys. Rev. Lett. **64**, 232 (1990).
- [23] A.B. Harris, T.C. Lubensky and E.J. Mele, Phys. Rev. B **40**, 2631 (1989);
D. Poilblanc and Y. Hasegawa, Phys. Rev. B **40**, 9035 (1989).
- [24] F.C. Zhang, Phys. Rev. Lett. **64**, 974 (1990).
- [25] D.N. Sheng, Z.B. Su, and L. Yu, Phys. Rev. B **42**, 8732 (1990).
- [26] F. Nori, E. Abrahams, and G.T. Zimanyi, Phys. Rev. B **41**, 7277 (1989);
see, also J.P. Rodrigues and B. Doucot, Europhys. Lett. **11**, 415 (1990).
- [27] P.A. Lee and N. Nagaosa, Phys. Rev. B. **46**, 5621 (1992).
- [28] H. Ding, *et al.*, Preprint cond-mat/9611194.
- [29] N.P. Ong, *et al.*, Phys. Rev. B **35**, 8807 (1987);
Y. Fukuzumi, K. Mitsuhashi, K. Takenada, and S. Uchida (to be published).
- [30] P.A. Marchetti, Z.B. Su, and L. Yu, Nucl. Phys. B **482**[FS], 731 (1996) and unpublished.

Figure Captions

Figure 1. Diagrammatic illustration of the π -flux state. A $\pi(-\pi)$ magnetic flux flows alternatively through neighboring plaquette of the lattice.

Figure 2. The comparison of the total free energy F for the coexisting π -flux + d-wave RVB state and the pure d-wave RVB state.

Figure 3. The unclosed pocket-like spinon Fermi surface at $\delta=0.2$. The four directions along which we calculate the physical electron spectral function are marked in the figure as α, β, γ_1 and γ_2 .

Figure 4. The momentum distribution of the spinons along the four directions defined in Fig.3.

Figure 5. The physical electron spectral function along the α cut, from which we see a clear Fermi-level crossing and no pseudo-gap.

Figure 6. The physical electron spectral function along the γ_1 cut. A pseudo-gap opens, but the Fermi-level crossing is still visible in this direction.

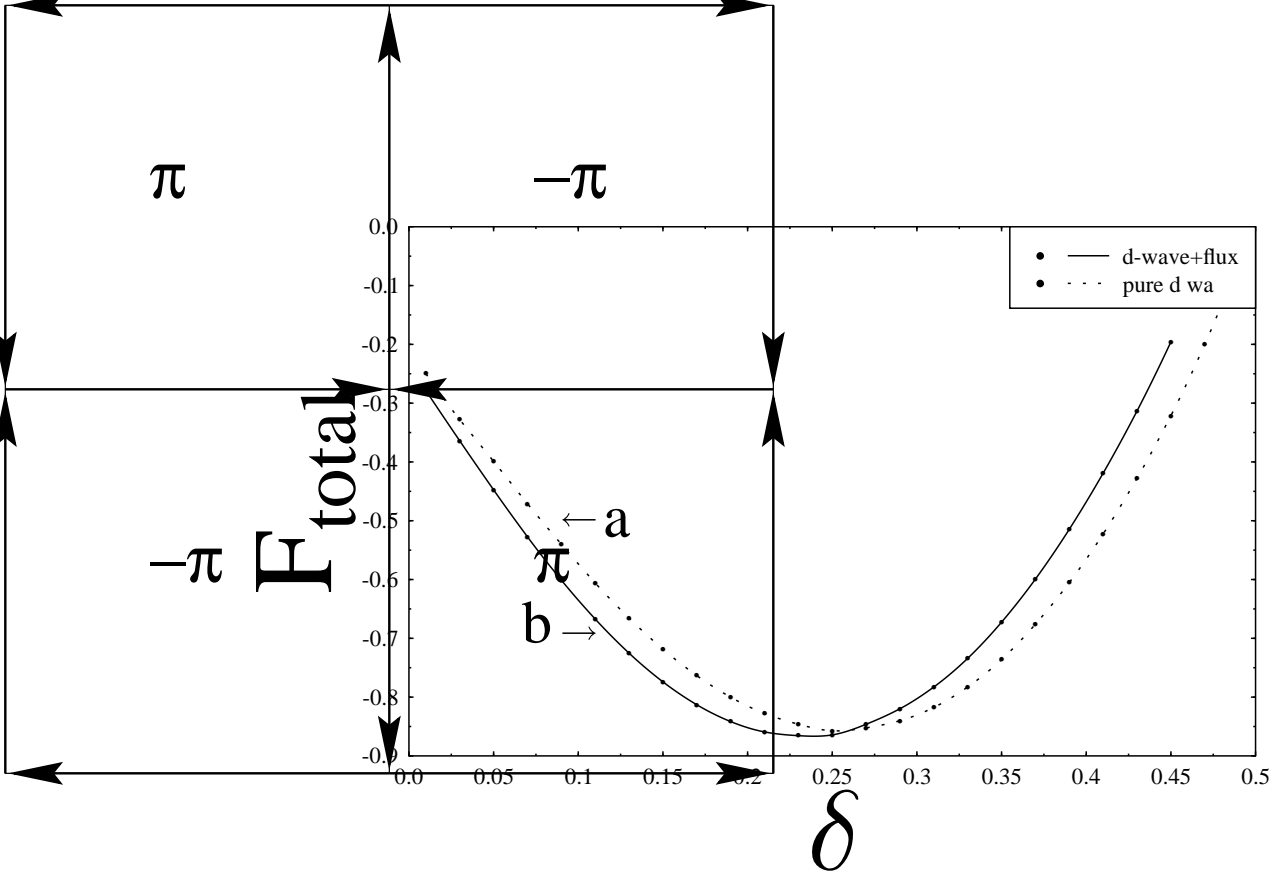


Fig.1

Fig.2

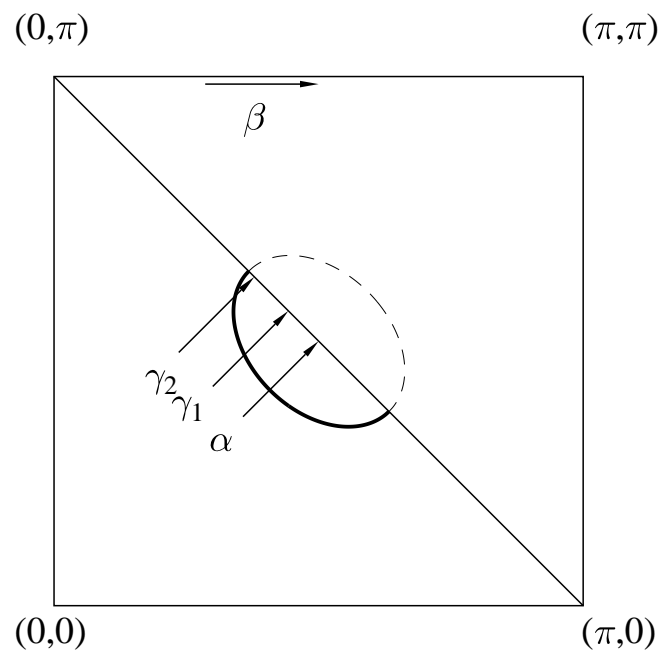


Fig.3

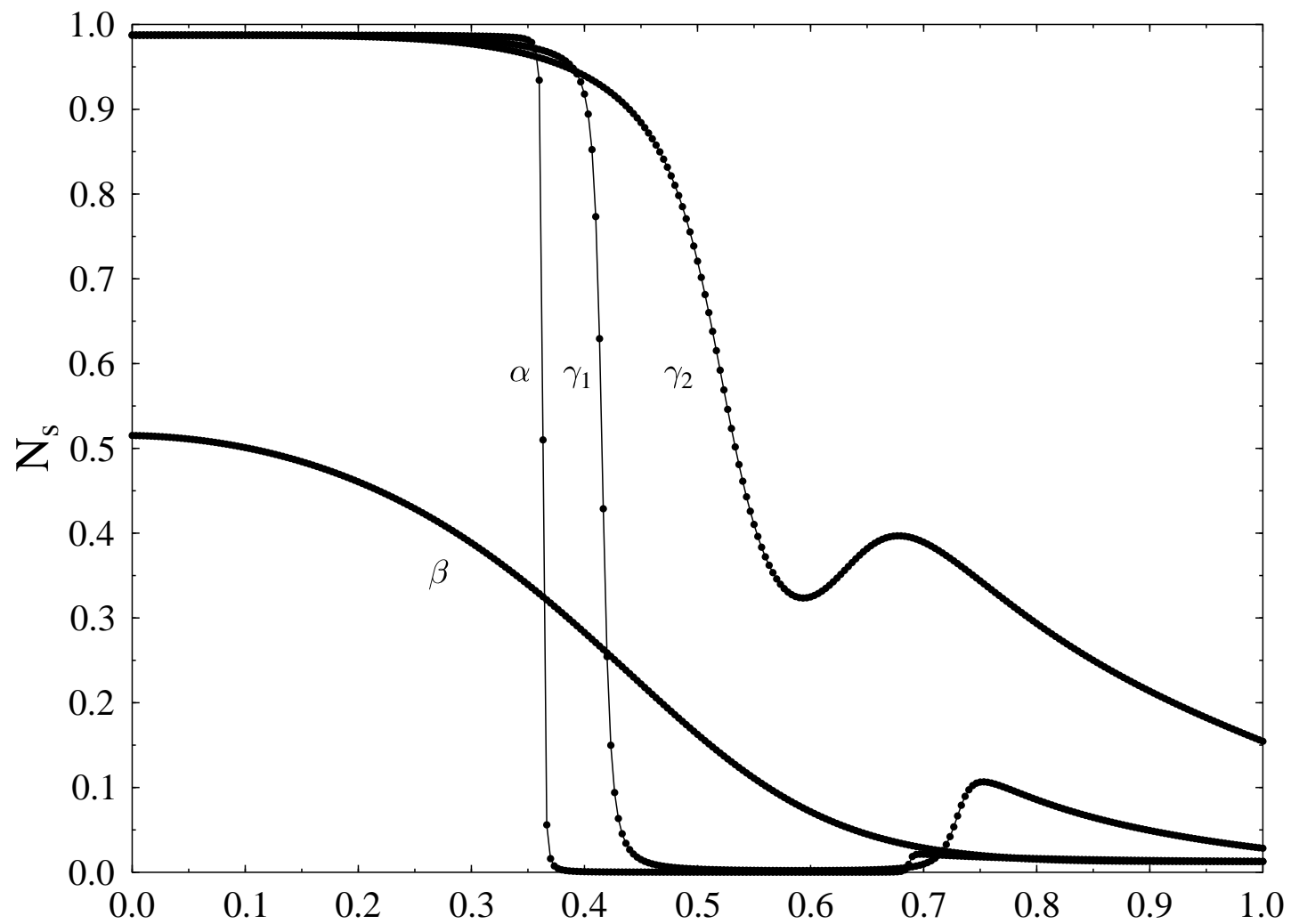


Fig.4

Fig.5.

Arbitrary unit

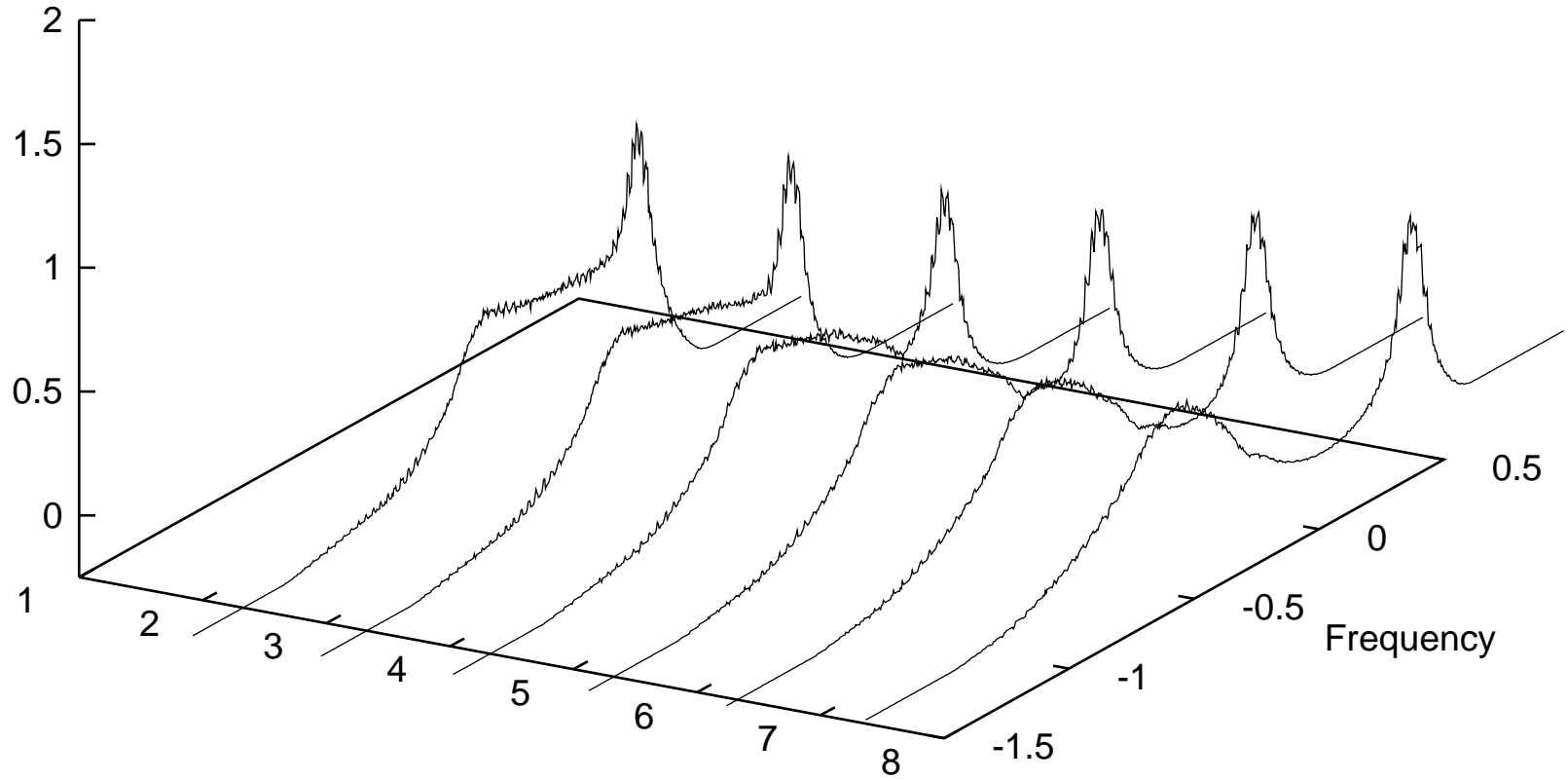


Fig.6.

Arbitrary unit

